

MOLECULAR GAS IN THE $z = 2.8$ SUBMILLIMETER GALAXY SMM 02399–0136

D. T. FRAYER¹, R. J. IVISON^{2,3}, N. Z. SCOVILLE¹, M. YUN⁴, A. S. EVANS¹, IAN SMAIL⁵, A. W. BLAIN⁶, AND J.-P. KNEIB⁷

Draft version December 9, 2017

ABSTRACT

We report the detection of CO(3→2) emission from the submillimeter-selected hyperluminous galaxy SMM02399–0136. This galaxy is the brightest source detected in the recent SCUBA surveys of the submillimeter sky. The optical counterpart of the submillimeter source has been identified as a narrow-line AGN/starburst galaxy at $z = 2.8$. The CO emission is unresolved, $\theta \lesssim 5''$, and is coincident in redshift and position with the optical counterpart. The molecular gas mass derived from the CO observations is $8 \times 10^{10} h_{75}^{-2} M_{\odot}$, after correcting for a lensing amplification factor of 2.5. The large CO luminosity suggests that a significant fraction of the infrared luminosity of SMM 02399–0136 arises from star formation. The high inferred star-formation rate of $10^3 M_{\odot} \text{ yr}^{-1}$ and the large gaseous reservoir may suggest that we are seeing the formation phase of a massive galaxy. Future CO observations of other galaxies detected in deep submillimeter surveys will test the generality of these conclusions for the bulk of the faint submillimeter population.

Subject headings: early universe — galaxies: active — galaxies: evolution — galaxies: individual (SMM 02399–0136) — galaxies: starburst

1. INTRODUCTION

Recent observational results have dramatically increased our knowledge of galaxy evolution at high redshift. Ultraviolet- and optically-selected samples of distant galaxies suggest that the star-formation rate per comoving volume in the Universe peaks at $z \sim 1-2$ (Madau et al. 1996, and references therein). The first results from deep surveys of the submillimeter sky (Smail, Ivison & Blain 1997; Blain et al. 1998; Barger et al. 1998; Hughes et al. 1998; Eales et al. 1998) using the Submillimeter Common-User Bolometer Array (SCUBA) on the James Clerk Maxwell Telescope may imply that a large proportion of the star formation at high redshift is obscured by dust at UV/optical wavelengths. Observations of CO and dust at high redshift are, hence, important for constraining the early evolution of galaxies.

Despite considerable observational effort, there are still only a few known high-redshift CO sources. These include IRAS F 10214+4724 (Brown & Vanden Bout 1991; Solomon, Downes, & Radford 1992), the Cloverleaf quasar H 1413+117 (Barvainis et al. 1994), BR 1202-0725 (Ohta et al. 1996; Omont et al. 1996), 53W002 (Scoville et al. 1997a), and BRI 1335-0417 (Guilloteau et al. 1997). In this *Letter*, we report the detection of CO(3→2) emission in submillimeter source SMM 02399–0136, hereafter SMM02399.

The galaxy SMM02399 is the brightest submillimeter source discovered during a survey through rich, lensing clusters (Smail et al. 1997). Follow-up optical work places SMM02399 at a redshift of $z = 2.803 \pm 0.003$, indicating

that the source is gravitationally amplified by the foreground cluster by a factor of 2.5 (Ivison et al. 1998; hereafter I98). The optical data show the presence of a bright compact source (L1) containing a narrow-line AGN, with an unknown contribution due to star formation, and a diffuse companion (L2) thought to be interacting or merging with L1 (I98). The submillimeter data are consistent with thermal dust emission and suggest a massive dust reservoir of order $10^8 M_{\odot}$ (I98).

2. OBSERVATIONS

SMM02399 was observed using the Owens Valley Millimeter Array in two configurations of six 10.4m telescopes. A total of 54.7 hours of usable integration time on source was obtained between January 1998 and May 1998. The phase center for the radio observations was the position of the brightest optical component of the SMM02399 system (L1); RA(J2000)=02^h39^m51^s.88; DEC(J2000)=−01°35′58″.0 (I98). The CO(3→2) line was observed using a digital correlator configured with 112×4 MHz channels. The receivers were initially tuned to 90.927 GHz, corresponding to CO(3→2) emission at the optical redshift of $z = 2.803$. The CO line was placed in the lower side-band (LSB) for which the receivers were optimized. Typical LSB system temperatures were approximately 300 K, corrected for telescope losses and the atmosphere. In addition to the CO line data, we recorded the 3mm continuum data with a 1 GHz bandwidth measured in both the lower and upper side-bands. The nearby quasar 0238–084 was observed every 25 minutes for gain

¹Astronomy Department, California Institute of Technology 105–24, Pasadena, CA 91125, USA

²Institute for Astronomy, Department of Physics & Astronomy, University of Edinburgh, Blackford Hill, Edinburgh, EH9 3HJ, UK

³Department of Physics & Astronomy, University College London, Gower Street, London, WC1E 6BT, UK

⁴National Radio Astronomy Observatory, P.O. Box 0, Socorro, NM 87801, USA

⁵Department of Physics, University of Durham, South Road, Durham, DH1 3LE, UK

⁶Cavendish Laboratory, Madingley Road, Cambridge, CB3 0HE, UK

⁷Observatoire Midi-Pyrénées, 14 Avenue E. Belin, F-31400 Toulouse, France

and phase calibration. Absolute flux calibration was determined from observations of Uranus and Neptune, resulting in a calibration uncertainty of about 15% for SMM02399.

3. RESULTS

Figure 1a shows the CO(3→2) spectrum for the data taken from 01 January to 17 April (38.3 hr). These data suggest that the CO emission is centered on a slightly higher redshift ($z \simeq 2.808$) than the optical redshift. We obtained follow-up observations from 28 April to 21 May (16.4 hr) with the spectrometer shifted to a central frequency of 90.815 GHz in order to obtain a complete profile for the CO emission line (Fig. 1b). Both data sets were combined to produce the cumulative CO(3→2) spectrum in Figure 1c. To produce the spectra, naturally-weighted image cubes were made by averaging the data over independent 24 MHz (79 km s⁻¹) channels. The resulting data cubes were then hanning smoothed, and a continuum level of 0.5 mJy (i.e., a DC offset) was subtracted from the data. All spectra were taken along the frequency axis of the image cubes at the position of the CO emission (Table 1).

Although the spectral-line data may suggest a weak continuum level, we lack the sensitivity to detect continuum emission from SMM02399. In the LSB continuum data we find a flux density of 0.9 ± 0.3 mJy which is consistent with only the CO emission averaged over the 1 GHz continuum bandwidth. From the upper-side band continuum data (line-free), we achieve an upper limit of $S(3\text{mm}) < 0.7$ mJy (1σ). For the remaining of the paper, we adopt the expected continuum level of 0.3 mJy, derived from extrapolating the previous submillimeter observations of thermal dust emission (I98).

Figure 2 shows the naturally-weighted channel maps averaged over independent 112 MHz channels. As stated earlier, the data were taken at two different frequencies. The rms noise level is higher for end channels A&E, since these contain less integration time than the central three channels. We detect CO emission at the optical position of SMM02399 in channels C&D. By averaging the data in channels C&D (224 MHz, 740 km s⁻¹), we achieve an 8σ detection (Fig. 2). We obtain an integrated flux of 3.3 ± 0.4 Jy km s⁻¹ and determine the CO source position (Table 1) by fitting a Gaussian to the peak in the integrated map. After subtracting the expected continuum level of 0.3 mJy, the resulting CO(3→2) line flux is $S(\text{CO}) = 3.0 \pm 0.4$ Jy km s⁻¹. By assuming a lensing amplification factor of 2.5, the observed CO(3→2) line flux implies intrinsic line luminosities of $L(\text{CO}) = 2.5 \times 10^7 h_{75}^{-2} L_{\odot}$ and $L'(\text{CO}) = 1.9 \times 10^{10} h_{75}^{-2} \text{K km s}^{-1} \text{pc}^2$ ($q_0 = 0.5$). $L'(\text{CO})$ is related to the mass of molecular gas (including He) by $M(\text{H}_2)/L'(\text{CO}) = \alpha$. We adopt a value of $\alpha = 4 M_{\odot} (\text{K km s}^{-1} \text{pc}^2)^{-1}$, which is similar to the Galactic value (e.g., Sanders, Scoville, & Soifer 1991), and infer a molecular gas mass of $M(\text{H}_2) \simeq 8 \times 10^{10} h_{75}^{-2} M_{\odot}$. The appropriate value for α is uncertain within a factor of 2–3. It has been argued that the Galactic value may overestimate the amount of molecular gas in ultraluminous galaxies (Solomon et al. 1997), while other factors such as sub-solar metallicities (Wilson 1995) and $T_b(3-2)/T_b(1-0)$ brightness temperature ratios less than unity (Devereux et al. 1994) lead to underestimates of the

molecular gas mass.

The CO emission seen in Figure 2 is unresolved. By varying the (u,v) weighting schemes and using deconvolution techniques, we find an upper-limit for the CO source size of $\theta < 5''$. This angular limit corresponds to a maximum linear diameter of $D < 25 h_{75}^{-1}$ kpc at $z = 2.8$, or $D < 10 h_{75}^{-1}$ kpc after correcting for lensing. We can use this limit to constrain the dynamical mass in SMM02399. The dynamical mass within the CO emission regions is $M_{\text{dyn}} = R(\Delta V/[2 \sin(i)])^2/G$, where ΔV is the observed line width of 710 km s⁻¹. The inclination is unknown. We find $M_{\text{dyn}} < 1.5 \times 10^{11} \sin^{-2}(i) h_{75}^{-1} M_{\odot}$. These results indicate a gas fraction of $M(\text{H}_2)/M_{\text{dyn}} > 0.5 \sin^2(i) h_{75}^{-1}$, which is consistent with a gas-rich young starburst.

4. DISCUSSION

The CO emission is positionally coincident with the SCUBA source SMM02399 and the compact optical counterpart (L1) within the uncertainties of the data sets (Fig. 2). The central frequency of the CO emission is slightly redshifted with respect to the mean redshift of the optical lines (400 km s⁻¹), but such offsets have been noted previously for low redshift luminous galaxies (Mirabel & Sanders 1988). These offsets have been interpreted as a signature of outflows in the optically emitting gas where the receding emission is obscured by dust (Mirabel & Sanders 1988). The CO emission is unresolved ($\theta < 5''$), unlike the Ly α emission and the 20 cm radio continuum emission which are $\theta \sim 8''$ in extent (I98). Since it is common for ultraluminous merger systems to be compact CO sources (Downes & Solomon 1998), it is not surprising that the CO emission for SMM02399 is unresolved. In addition, the broad CO line, with an apparent double peak profile, is consistent with the suspected merger scenario for the system (I98).

The derived molecular gas mass of approximately $10^{11} M_{\odot}$ for SMM02399 is about 50 times higher than the Milky Way (Solomon & Rivolo 1989) and is a few times more massive than the most luminous low redshift infrared galaxies (Sanders et al. 1991). The high molecular gas mass observed in SMM02399 is not unique for high-redshift systems. Other high-redshift CO sources have similarly large molecular gas masses (e.g., Guilleoteau et al. 1997), and this may indicate evolution in $M(\text{H}_2)$. Such increases are expected in simple theoretical models (Frayer & Brown 1997). However, given the uncertainties in α (Solomon et al. 1997), the lensing uncertainties, and the small number of high-redshift CO sources, the possibility of evolution is only a suggestion at the present time.

We derive a gas to dust ratio of $M(\text{H}_2)/M(\text{dust}) \simeq 140\text{--}700$ for SMM02399, assuming a range of dust temperatures of 30–70 K. This gas to dust ratio is similar that found for other high-redshift CO sources and is also similar to that observed in nearby galaxies (Devereux & Young 1990). This consistency suggests that the high-redshift CO sources are already significantly chemically evolved. Based on the deficient CO luminosities observed in metal-poor galaxies (e.g., Sage et al. 1992), the $L'(\text{CO})/L(1.25\text{mm})$ luminosity ratios for the high-redshift CO sources are consistent with metallicities of $Z \gtrsim 0.2 Z_{\odot}$.

The SCUBA measurements indicate that SMM02399 is a hyperluminous infrared galaxy (HyLIG, as defined by

Sanders & Mirabel 1996), and the optical data suggest the presence of both a dust-enshrouded AGN and starburst activity (I98). An important unanswered question is which mechanism is responsible for the majority of its immense infrared luminosity. The relative importance of AGN and starburst activity seen in even the nearest ultraluminous galaxies is still uncertain (e.g., Scoville, Yun, & Bryant 1997b; Downes & Solomon 1998). Based on observations using the Infrared Space Observatory, Genzel et al. (1998) find that about 25% of ultraluminous galaxies are powered by AGNs, while the remaining 75% are dominated by star formation. It is not clear if this trend will hold for the HyLIGs.

The detection of CO in SMM02399 suggests the importance of star formation by showing the presence of a massive reservoir of molecular gas from which stars are formed. Other HyLIG galaxies which do not show CO have extremely high $L(\text{IR})/L'(\text{CO})$ ratios and are thought to be dominated by AGN activity (Evans et al. 1998). The $L(\text{IR})/L'(\text{CO})$ ratio for SMM02399, on the other hand, is roughly consistent with that found for luminous starbursts (Sanders & Mirabel 1996). After correcting for the lensing of SMM02399, we find a far-infrared (FIR) luminosity (Helou et al. 1988) of $L(\text{FIR}) = 1.2 \times 10^{13} h_{75}^{-2} L_{\odot}$ and a ratio of $L(\text{FIR})/L'(\text{CO}) = 630 L_{\odot} (\text{K km s}^{-1} \text{pc}^2)^{-1}$. For comparison, the ultraluminous putative starburst galaxy Arp 220 has a $L(\text{FIR})/L'(\text{CO})$ ratio which is only about a factor of 2 lower.

The starburst nature of SMM02399 is further supported by the far-infrared to 4.85 GHz radio flux ratio parameter q (Condon, Frayer, & Broderick 1991)⁸. For SMM02399 we find $q = 2.3$ which is similar to, but lower than, the mean value of $\langle q \rangle = 2.64 \pm 0.16$ observed in nearby starburst galaxies (Condon et al. 1991). Although the data for SMM02399 show the importance of star formation, the data also suggest that the AGN activity is not negligible. For pure star formation, we would expect a higher q value and a lower $L(\text{FIR})/L'(\text{CO})$ ratio. In summary,

the current data are consistent with $50 \pm 25\%$ of the infrared luminosity being powered by star formation, with the remaining fraction due to the AGN.

Assuming that half of the infrared luminosity of SMM02399 is powered by star formation, the implied star formation rate for massive stars is $\text{SFR}(M > 5 M_{\odot}) \simeq 550 M_{\odot} \text{yr}^{-1} h_{75}^{-2}$, using the relationship given by Condon (1992). Including low mass stars, we expect a total SFR of order $10^3 M_{\odot} \text{yr}^{-1}$, depending on the details of the IMF. Although high, this SFR is below the maximum allowable rate permitted for the observed CO line width (Lehnert & Heckman 1996).

5. CONCLUSIONS

We report the first detection of CO in a distant galaxy, SMM02399, discovered during the recent deep surveys of the submillimeter sky. The CO emission is coincident in position and redshift with the optical counterpart of SMM02399. The CO observations indicate the presence of $8 \times 10^{10} h_{75}^{-2} M_{\odot}$ of molecular gas. Comparison of the properties of SMM02399 with local starbursts suggests that star formation accounts for approximately 25–75% of its immense infrared luminosity, with remaining contribution coming from an AGN. The derived star-formation rate is of order $10^3 M_{\odot} \text{yr}^{-1}$. Similar observations of other high-redshift submillimeter sources will test whether the properties of SMM02399 are representative of the general faint submillimeter population, as well as placing limits on the contribution of dust-enshrouded AGN to the extragalactic submillimeter background.

We thank our colleagues at the Owens Valley Millimeter Array who have helped make these observations possible. The Owens Valley Millimeter Array is a radio telescope facility operated by the California Institute of Technology and is supported by NSF grants AST 93-14079 and AST 96-13717. RJI and IRS acknowledge support from PPARC Advanced Fellowships.

REFERENCES

- Barger, A. J., et al. 1998, *Nature*, in press (astro-ph/9806317)
 Barvainis, R., Tacconi, L., Antonucci, R., Alloin, D., & Coleman, P. 1994, *Nature*, 371, 586
 Blain, A. W., Smail, I., Ivison, R. J., & Kneib, J.-P. 1998, *MNRAS*, submitted (astro-ph/9806062)
 Brown, R. L., & Vanden Bout, P. A. 1991, *AJ*, 102, 1956
 Condon, J. J. 1992, *ARA&A*, 30, 575
 Condon, J. J., Frayer, D. T., Broderick, J. J. 1991, *AJ*, 101, 362
 Devereux, N., Taniguchi, Y., Sanders, D. B., Nakai, N., & Young, J. S. 1994, *AJ*, 107, 2006
 Devereux, N. A., & Young, J. S. 1990, *ApJ*, 359, 42
 Downes, D. & Solomon, P. M. 1998, *ApJ*, in press (astro-ph/9806377)
 Eales, S. et al. 1998, *ApJ*, submitted (astro-ph/9808040)
 Evans, A. S., et al. 1998, *ApJ*, in press (astro-ph/9806091)
 Frayer, D. T., & Brown, R. L. 1997, *ApJS*, 113, 221
 Genzel, R., et al. 1998, *ApJ*, 498, 579
 Guilloiseau, S., Omont, A., McMahon, R. G., Cox, P., & Petitjean, P. 1997, *A&A*, 328, L1
 Helou, G., Khan, I. R., Malek, L., & Boehmer, L. 1988, *ApJS*, 68, 151
 Hughes, D., et al. 1998, *Nature*, in press (astro-ph/9806297)
 Ivison, R. J. et al. 1998, *MNRAS*, 298, 583 (I98)
 Kneib, J.-P., Mathez, G., Fort, B., Mellier, Y., Soucaill, G., & Longaretti, P.-Y. 1994, *A&A*, 286, 701
 Lehnert, M. D., & Heckman, T. M. 1996, *ApJ*, 472, 546
 Madau, P., Ferguson, H. C., Dickinson, M. E., Giavalisco, M., Steidel, C. S., & Fruchter, A. 1996, *MNRAS*, 283, 1388
 Mirabel, I. F., & Sanders, D. B. 1988, *ApJ*, 335, 104
 Ohta, K., Yamada, T., Nakanishi, K., Kohno, K., Akiyama, M., & Kawabe, R. 1996, *Nature*, 382, 426
 Omont, A., Petitjean, P., Guilloiseau, S., McMahon, R. G., Solomon, P. M., & Pécontal, E. 1996, *Nature*, 382, 428
 Sage, L. J., Salzer, J. J., Loose, H.-H., & Henkel, C. 1992, *A&A*, 265, 19
 Sanders, D. B., & Mirabel, I. F. 1996, *ARA&A*, 34, 749
 Sanders, D. B., Scoville, N. Z., & Soifer, B. T. 1991, *ApJ*, 370, 158
 Scoville, N. Z., Yun, M. S., Bryant, P. 1997b, *ApJ*, 484, 702
 Scoville, N. Z., Yun, M. S., Windhorst, R. A., Keel W. C., & Armus, L. 1997a, *ApJ*, 485, L21
 Smail, I., Ivison, R. J., & Blain, A. W. 1997, *ApJ*, 490, L5
 Solomon, P. M., Downes, D., & Radford, S. J. E. 1992, *ApJ*, 398, L29
 Solomon, P. M., Downes, D., Radford, S. J. E., & Barrett, J. W. 1997, *ApJ*, 478, 144
 Solomon, P. M., & Rivolo, A. R. 1989, *ApJ*, 339, 919
 Wilson, C. D. 1995, *ApJ*, 448, L97

⁸We use a q parameter based on the 4.85 GHz radio flux densities instead of the more often cited q parameter based on a radio frequency 1.4 GHz, since the radio rest-frame frequency observed for SMM02399 is 5.3 GHz (I98).

TABLE 1
CO OBSERVATIONAL RESULTS

| Parameter | Value |
|-------------------------------------|---|
| RA (J2000) | $02^{\text{h}}39^{\text{m}}51^{\text{s}}.89 \pm 0^{\text{s}}.02$ |
| DEC (J2000) | $-01^{\circ}35'58''.9 \pm 0''.5$ |
| $\langle z(\text{CO}) \rangle$ | 2.808 ± 0.002 |
| $\Delta V(\text{CO})_{\text{FWHM}}$ | $710 \pm 80 \text{ km s}^{-1}$ |
| $S(\text{CO})^{\text{a}}$ | $3.0 \pm 0.4 \text{ Jy km s}^{-1}$ |
| $L(\text{CO})^{\text{b}}$ | $2.5 \times 10^7 h_{75}^{-2} L_{\odot}$ |
| $L'(\text{CO})^{\text{b}}$ | $1.9 \times 10^{10} h_{75}^{-2} \text{ K km s}^{-1} \text{ pc}^2$ |
| $M(\text{H}_2)^{\text{b,c}}$ | $8 \times 10^{10} h_{75}^{-2} M_{\odot}$ |

^aObserved CO(3→2) line flux assuming a continuum level of 0.3 mJy.

^bIntrinsic value assuming a lensing amplification factor of 2.5, $q_o = 0.5$, and $H_o = 75 h_{75} \text{ km s}^{-1} \text{ Mpc}^{-1}$.

^cEstimated using $\alpha = 4 M_{\odot} (\text{K km s}^{-1} \text{ pc}^2)^{-1}$.

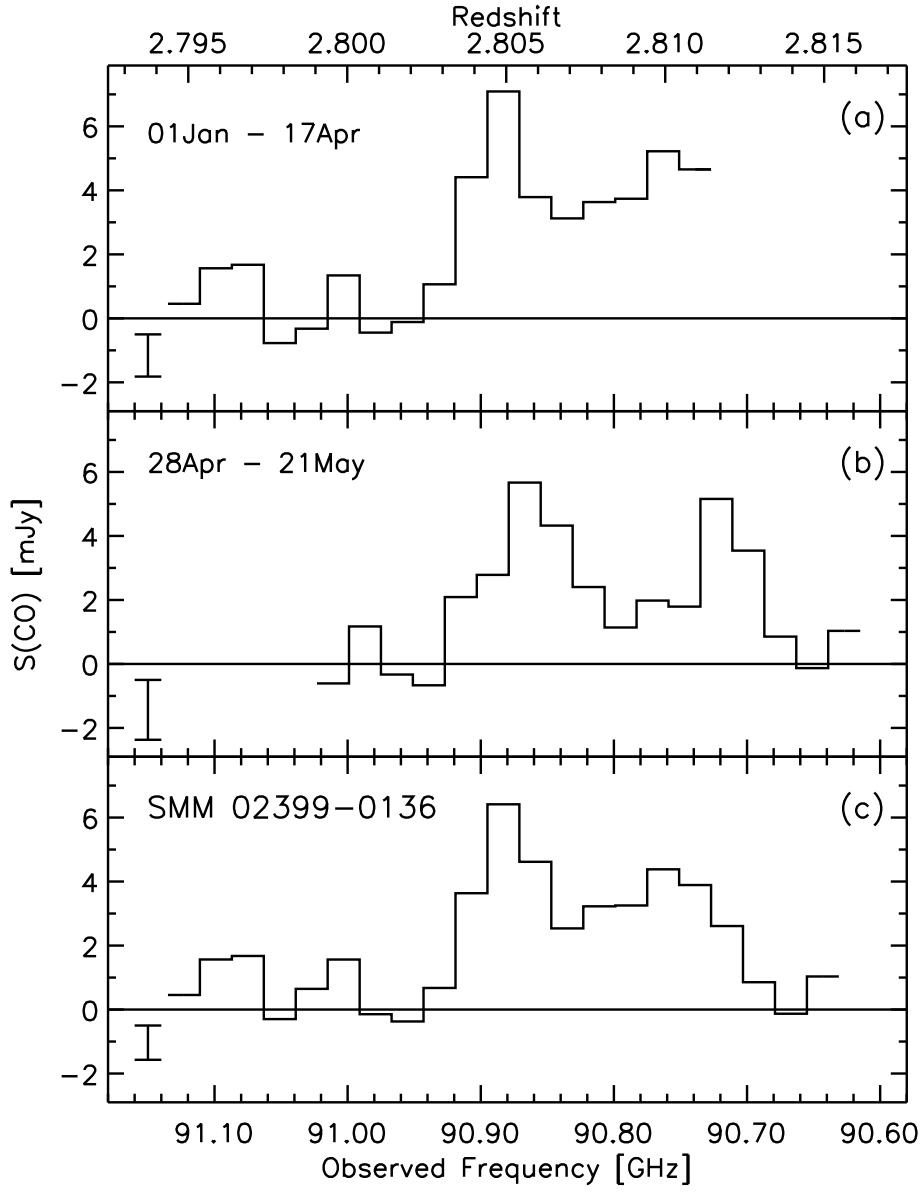


FIG. 1.— The CO(3→2) spectra for SMM02399 observed with the OVRO Millimeter Array. Panels (a)&(b) show subsets of the data, while panel (c) displays the cumulative spectrum. The 1σ error bar is shown in the lower left of each panel.

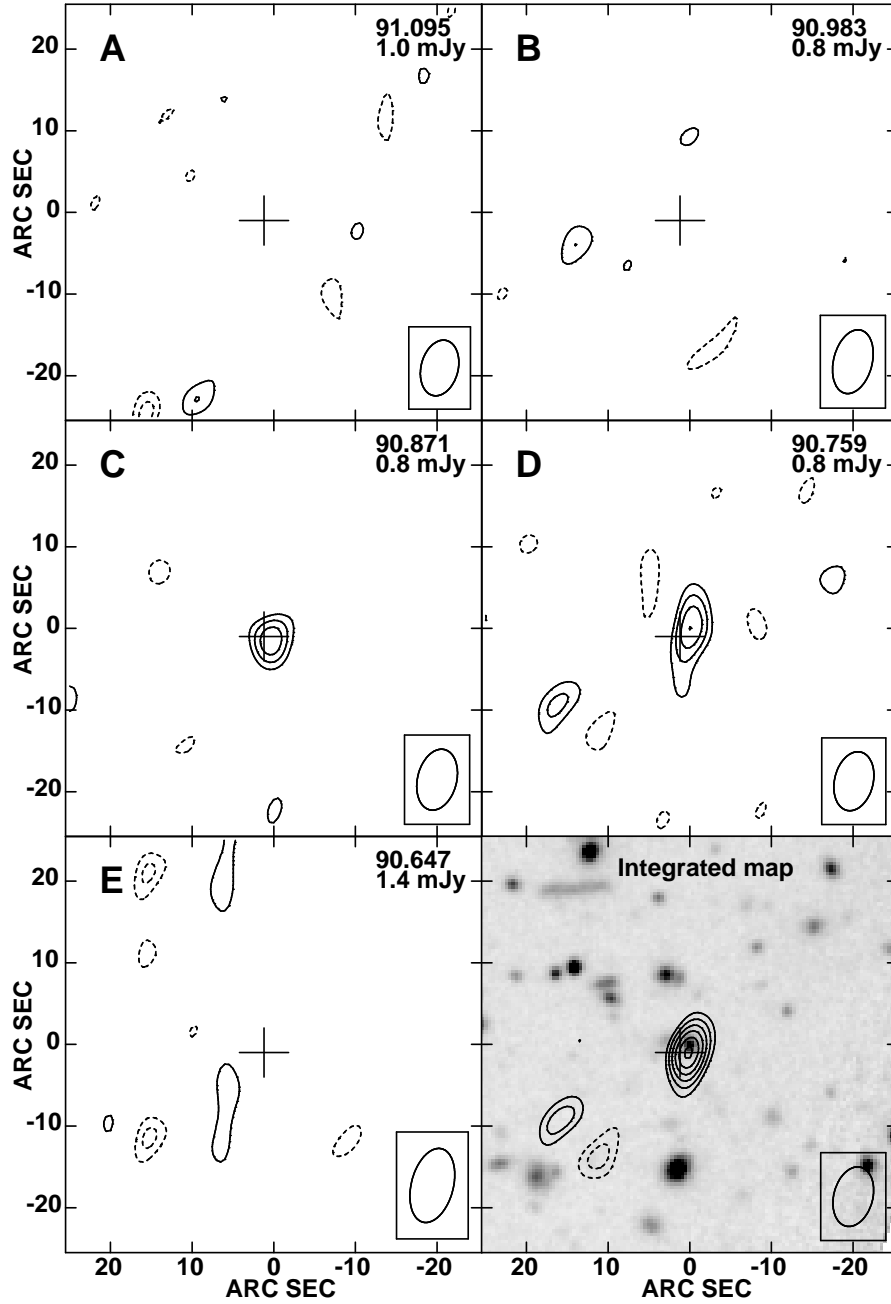


FIG. 2.— In panels A–E we show the CO(3→2) channel maps averaged over 112 MHz. The observed central frequency in GHz and the 1σ rms level of each channel are given in the top right. The positional offsets are relative to the optical position (north is at the top, and east is at the left), and the SCUBA position (198) is shown by a cross. The contour levels are $1\sigma \times (-3.5, -2.5, 2.5, 3.5, 4.5, 5.5)$ in panels A–E. In the lower right panel is the integrated CO map averaged over 224 MHz (channels C&D) overlaid on an optical B-band image taken with the Canada–France–Hawaii Telescope (Kneib et al. 1994). The 1σ rms level is 0.4 Jy km s^{-1} , and the contour levels are $1\sigma \times (-4, -3, 3, 4, 5, 6, 7, 8)$. The upper limit to the 3mm continuum level is 0.5 Jy km s^{-1} in the integrated map. The synthesized beam size is shown in the lower right ($7''.4 \times 4''.8$, PA = -15°).